Supplementary Information

Quantitative Nanometer-Scale Characterization of Densification in Fused Silica via s-SNOM

Ying Yan,*[a] Bo Jiang, [a] Qing Mu, [a] and Ping Zhou [a]

[a] *State Key Laboratory of High-performance Precision Manufacturing, Department of Mechanical Engineering, Dalian University of Technology, Dalian 116024, China*

Corresponding author. Email: yanying@dlut.edu.cn

1. Finite Dipole Model.

According to the principle of s-SNOM, the amplitude and phase signals obtained are directly determined by the scattering coefficients, and the scattering coefficient σ can be described as the ratio of scattered field strength (E_s) to incident field strength (E_i): [1]

$$\sigma \propto E_s / E_i. \tag{S1}$$

The relationship between the amplitude (S) and phase (φ) signals of s-SNOM and the scattering coefficient can be described as

$$\sigma = S \cdot e^{i\varphi}. \tag{S2}$$

The interaction between the tip and the sample is primarily a mutual polarization process, usually represented by the effective polarizability α_{eff}. The relationship between the scattering coefficient and effective polarizability is:

$$\sigma = (1+r)^2 \alpha_{eff}, \tag{S3}$$

where r is the far-field reflection coefficient. In the FDM, the relationship between effective polarizability and system parameters is given by: [1,2]

$$\alpha_{eff} = 1 + \frac{1}{2}\frac{f_0(H)\beta(\varepsilon)}{1 - f_1(H)\beta(\varepsilon)}, \tag{S4}$$

where f_i(H) is the geometry factors which depends on the radius of the tip R, spheroid major half-axis length L and distance between the tip and simple H, β is the quasi-

electrostatic reflection coefficient of the sample. f_0(H), f_1(H), β, and H can be expressed as:

$$f_0 = \left(g - \frac{R + 2H + W_0}{2L} \right) \cdot \frac{\ln \frac{4L}{R + 4H + 2W_0}}{\ln \frac{4L}{R}}, \tag{S5}$$

$$f_1 = \left(g - \frac{R + 2H + W_1}{2L} \right) \cdot \frac{\ln \frac{4L}{2R + 4H}}{\ln \frac{4L}{R}}, \tag{S6}$$

$$\beta = \frac{\varepsilon - 1}{\varepsilon + 1}, \tag{S7}$$

$$H = A\left(1 + \cos \Omega t\right), \tag{S8}$$

$$W_0 \approx \frac{1.31RL}{L + 2R}, \tag{S9}$$

$$W_1 \approx \frac{R}{2}, \tag{S10}$$

where ε is the dielectric constant of the sample, g represents the amount of induced charge, W_0 represents the distance of charge Q_0 from the bottom of the tip axis and W_1 represents the distance of charge Q_1 from the bottom of the tip axis. In this study, the amount of induced charge g=0.7exp(0.6i), the radius of tip R=30 nm, spheroid major half-axis length L =300 nm, and the tapping amplitude A=50 nm.

To enhance the accuracy of signals obtained using FDM and to suppress the influence of background noise, high-order harmonic demodulation is applied to the near-field signal. The method is to take n_{th} Fourier coefficients at time t to obtain n_{th} demodulation scattering coefficients: [3]

$$\sigma_n = \left(1 + r\right)^2 \hat{F}_n \left[1 + \frac{1}{2} \frac{f_0\left(H\right)\beta\left(\varepsilon\right)}{1 - f_1\left(H\right)\beta\left(\varepsilon\right)} \right], \tag{S11}$$

2. Result of different harmonic demodulation order.

As the harmonic demodulation order increases, the scattered field of the background can be effectively removed. However, if the harmonic demodulation order n is too large, the detected near-field signal will be weak and the signal-to-noise ratio (SNR) will be deteriorated.

Therefore, it is necessary to find a balance point between minimizing background noise and maintaining a good SNR. [4,5] Fig. S1 shows the comparison of near-field signals at different harmonics for the 250 mN indentation. The amplitude signal increases significantly compared to the third harmonic. However, the phase signal becomes weaker, indicating that more far-field signals are detected. Therefore, the harmonic demodulation order *n* is 3 in this study.

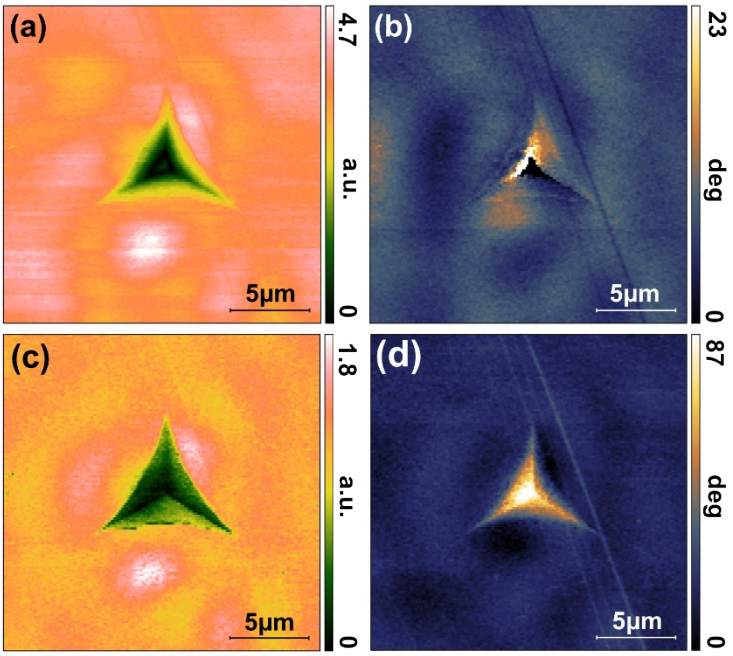

Fig. S1. Near-field amplitude and phase diagrams of 250 mN indentation at 1070 cm^{-1}: (a)-(b) show the second harmonic; (c)-(d) show the third harmonic.

3. Near-field optical results after etching

The etching solution was composed of 80 wt% DI water, 15 wt% NH4F and 5 wt% HF, and the etching rate of the polished surface of fused silica was measured at about 60 nm/min. The etching time was 4 minutes and the samples were pre-etched 10 nm to avoid the influence of contamination before measurements. Fig. S2a in the response shows the morphology of the indentation after etching. Compared with the unetched indentation, the densified area of the etched indentation is removed and the morphology changes significantly. Since the degree of densification at the edge of the indentation is low and the etching speed is different from that inside the indentation, pits appear at the edge of the indentation. The surface morphology also deteriorates after etching. Fig. S2b and Fig. S2c in the response show the amplitude and phase of the indentation after etching. The results show that after the densification is removed, only

in the area where the morphology changes rapidly, the amplitude and phase will have weak artifacts, such as the pits at the edge. The morphology inside the indentation changes gradually, and there are almost no artifacts in the amplitude and phase.

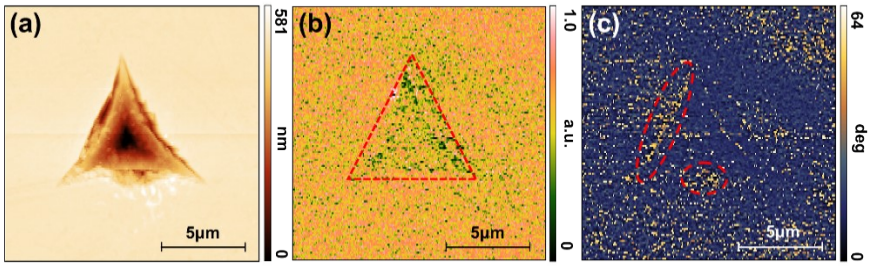

Fig. S2 (a) Morphology; (b) Amplitude; (c) Phase

It is worth noting that the morphology of all indentations in the manuscript changes gradually to the lowest level, without rapid changes in a small range. Therefore, the morphology changes in this study have no effect on the near-field optical test.

4. Computational results of the s-SNOM amplitude.

Fig S3 shows the comparison between the calculated and experimental results of amplitude. As the distance from the center of the indentation increases, the trends of the experimental and calculated results of amplitude differ significantly. In particular, the calculated results exhibited almost linear variation. However, the experimental data for the amplitude show a slow increase, followed by a rapid rise, and then another slow increase.

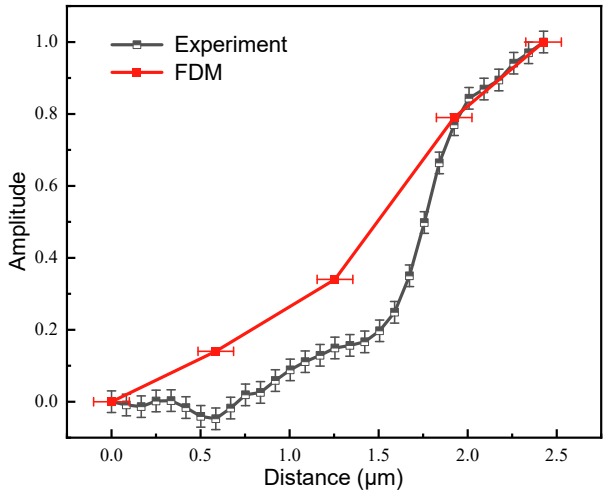

Fig S3 Comparison of near-field amplitude between the experimental and calculated results.

References

1 A. vitkovic, N. Ocelic, and R. Hillenbrand, *Opt. Express*., 2007, **15**, 8550-8565.

2 Ocelic, N. Quantitative Near-field Phonon-Polariton Spectroscopy, Technische Universität München, 2007.

3 A. A. Govyadinov, I. Amenabar, F. Huth, P. S. Carney and R. Hillenbrand, *J. Phys. Chem. Lett.*, 2013, **4**, 1526–1531.

4 A. A. Govyadinov, S. Mastel, F. Golmar, A. Chuvilin, P. S. Carney and R. Hillenbrand, *ACS Nano.*, 2014, **8**, 6911–6921.

5 C. Moreno, J. Alda, E. Kinzel and G. Boreman, *Appl. Opt.*, 2017, **56**, 1037-1045.